Korean J. Chem. Eng., **30**(4), 955-962 (2013)
DOI: 10.1007/s11814-012-0224-8

Determination of kinetic parameters during the thermal decomposition of epoxy/carbon fiber composite material

Jae Hun Lee*,*, Kwang Seok Kim**, and Hyo Kim***,†**

*Safety Research Division, Institute of Gas Safety R&D, Gyeonggi-do 429-712, Korea
**Korea Institute of Science and Technology (KIST), Seongbuk-gu, Seoul 136-791, Korea
***Department of Chemical Engineering, The University of Seoul, Dongdaemun-gu, Seoul 130-743, Korea
(*Received 14 April 2012 • accepted 22 December 2012*)

Abstract−An in-depth study to determine the thermal decomposition kinetics parameters such as the activation energy E_a, the reaction order n, and the pre-exponential factor A of epoxy/carbon fiber composite material has been conducted. We employ not only the modified peak property method that is proposed here, but also the conventional method in analyzing the experimental data, and compare the results to show the performance of the proposed model. The pyrolysis tests for the epoxy/carbon fiber composite materials are conducted by using thermogravimetric analyser at various heating rates. As a result, the best prediction to the experimental data can be obtained by the modified peak property method. Besides, among the methods applied here, the modified peak property method provides most convenient way to recover the parameters: it does not require a curve fitting of the data nor a long iterative computation.

Key words: Kinetic Parameters, Modified Peak Property Method, Epoxy/Carbon Fiber, TGA

INTRODUCTION

The current natural gas vehicles or fuel cell vehicles are equipped with a filament-wound, carbon/epoxy composite laminate overwrapped cylinder, i.e., composite cylinder, for the fuel storage purpose. Due to the light weight and good mechanical properties, the composite cylinder is considered a promising alternative to metal tanks. Nevertheless, there is still a very serious concern that safety is not yet guaranteed when a composite cylinder is involved in a fire accident. Unlike a metal cylinder, the epoxy resin in the composite cylinder decomposes as it is exposed to a flame. The thermal decomposition causes the cylinder wall to be weakened and thus the mechanical strength of the cylinder becomes deteriorated. In the meantime, heat that is continuously transferred into the cylinder leads to an increase in vapor pressure of liquid fuel. Ultimately, the scenario ends up with a catastrophic accident.

To avoid such a dangerous accident and relieve the safety concerns, a safety margin must be considered in the design of the cylinder to predict and control the breakdown. To this end, repeated fire exposure burst tests with a fuel-filled tank may be required. However, the experiment involves an extreme pressure up to 70 MPa, which is so dangerous that there are many technical and cost-related difficulties, such as securing enough space and protective equipment. Fortunately, such a difficulty can be often circumvented by modeling and simulation efforts replacing dangerous experimental trials. At this occasion, the validity of those indirect experiments can be guaranteed only by knowing the fundamentals of underlying mechanism, i.e., accurate values of the kinetic parameters.

For instance, Arrhenius-type kinetics is most widely adopted for quantifying the thermal decompositions of various composite materials, e.g., phenolic/carbon, epoxy/carbon, and polyester/glass fiber [1-6]. Arrhenius-type kinetics contains three parameters: activation energy E_a, reaction order n, and pre-exponential factor A.

For recovering the values of those parameters, burning profiles of specimens obtained from TGA are used. Once TGA data are collected, they can be gone through in three different ways: multi-curves, single-curve, and peak property methods (PPM). The multi-curves method (implemented by Ozawa [7], Friedman [8], and Kissinger [9]) leads to the values that are dependent on degree of decomposition, but error from ignoring the effect of heating rate may occur. The single curve method (used by Coats-Redfern [10,11]) can provide the simplest model to get the parameter since the choice of the reaction order is somehow arbitrary, that is, not directly related to the obtained data. Both require a curve fitting procedure of TGA data obtained. On the other hand, PPM takes advantage of properties at a peak of derivative thermogravimetry (DTG) curve. It does not require curve fitting [12-14], but root finding of nonlinear algebraic equations [15,16]. Note that, before PPM is systematically established, there have been attempts to estimate the kinetic parameters using the peak properties: degree (α_m) and rate (a.k.a height, H_m) of decomposition, and temperature (T_m) measured where the peak is located [17,18]. In those cases, curve fitting has been employed.

In this study, we've modified the conventional PPM so that curve fitting or iteration is not necessary at all. The detailed procedure of the modified method will be addressed later. The above four protocols for recovering the kinetic parameters are quantitatively evaluated and compared with one another by using the TGA data of epoxy/carbon fiber specimen.

MATERIALS AND METHODS

1. Chemical Reaction Kinetics Model

In the analysis on the thermal decomposition of the epoxy/carbon

†To whom correspondence should be addressed.
E-mail: hkim@uos.ac.kr

fiber composite specimen using the various instruments such as TGA or Differential Scanning Calorimeter (DSC), it is useful to define the degree of decomposition, α, as the fraction that has been degraded so far:

$$\alpha = \frac{(m_i - m)}{(m_i - m_f)}. \tag{1}$$

where m is the mass of sample, and the subscript i and f denote the initial and final states, respectively. The rate of change in α is known directly proportional to the n-th power of the undecomposed fraction, i.e., $1-\alpha$, such that

$$\frac{d\alpha}{dt} = k(1-\alpha)^n. \tag{2}$$

Like much of reaction kinetics, the rate constant k is a function of absolute temperature T, and is expressed by an Arrhenius-type equation:

$$k(T) = A\exp\left(-\frac{E_a}{RT}\right). \tag{3}$$

Here, A is a pre-exponential factor, E_a is the activation energy of decomposition reaction, and R is the gas constant (=8.314 J/mol K).

The substitution of Eq. (3) into Eq. (2) yields

$$\frac{d\alpha}{dt} = A\exp\left(-\frac{E_a}{RT}\right)(1-\alpha)^n. \tag{4}$$

And dividing both sides of Eq. (4) by the heating rate dT/dt (=β) in K/min gives

$$\frac{d\alpha}{dT} = \frac{A}{\beta}\exp\left(-\frac{E_a}{RT}\right)(1-\alpha)^n. \tag{5}$$

Eq. (5) can be integrated by the separation of variables method such that

$$g(\alpha) = \int_0^{\alpha}\frac{d\alpha}{(1-\alpha)^n} = \frac{A}{\beta}\int_{T_i}^{T_f}\exp\left(-\frac{E_a}{RT}\right)dT, \tag{6}$$

and, the result of Eq. (6) is solved for α to get

$$\alpha = 1-\exp\left[\frac{1}{(1-n)}\ln\left\{1-(1-n)\int_{T_i}^{T_f}\frac{A}{\beta}\exp\left(-\frac{E_a}{RT}\right)dT\right\}\right]. \tag{7}$$

Now, the degree of decomposition is expressed as a function of temperature.

2. Modified Peak Property Method

Like the conventional PPM, in the modified one, the quantities when the rate of change in alpha (i.e., DTG curve) hits the maximum as well.

$$H_m = \left(\frac{d\alpha}{dT}\right)_m = \frac{A}{\beta}\exp\left(-\frac{E_a}{RT}\right)(1-\alpha_m)^n. \tag{8}$$

where α_m and T_m are the degree of decomposition and the temperature when the rate of change in α is at the maximum. It can be found by setting the first derivative of Eq. (4) with respect to time equal to zero:

$$\frac{d}{dt}\left(\frac{d\alpha}{dt}\right) = \frac{d\alpha}{dt}\left[\frac{E_a\beta}{RT^2} - A\exp\left(-\frac{E_a}{RT}\right)n(1-\alpha)^{n-1}\right] = 0. \tag{9}$$

The rearrangement of Eq. (9) gives [9]

$$\ln\left(\frac{\beta}{T_m^2}\right) = \ln\left(n(1-\alpha_m)^{n-1}\frac{AR}{E_a}\right) - \frac{E_a}{RT_m}. \tag{10}$$

Then, the substitution of Eq. (10) back into Eq. (8) and the further rearrangement produces

$$E_a = \frac{nRT_m^2H_m}{(1-\alpha_m)}. \tag{11}$$

And the pre-exponential factor A is obtained from

$$A = \frac{H_m\beta}{\exp\left(-\frac{E_a}{RT_m}\right)(1-\alpha_m)^n}. \tag{12}$$

An alternate way for E_a calculation is used by Flynn and Wall [19] under the assumption that α_m is a weak function of β at $(d\alpha/dT)_m$:

$$\begin{aligned} E_a &= R\left(\frac{T_{m2}T_{m1}}{T_{m1}-T_{m2}}\right)\ln\left[\left(\frac{\beta_1}{\beta_2}\right)\left(\frac{T_{m2}}{T_{m1}}\right)^2\right]\left(\frac{1-\alpha_{m2}}{1-\alpha_{m1}}\right)^{n-1} \\ &\approx R\left(\frac{T_{m2}T_{m1}}{T_{m1}-T_{m2}}\right)\ln\left[\left(\frac{\beta_1}{\beta_2}\right)\left(\frac{T_{m2}}{T_{m1}}\right)^2\right]. \end{aligned} \tag{13}$$

where the subscripts 1 and 2 represent the peak properties at two distinct heating rates. However, Eq. (13) is not a good method since E_a does not reveal unique value by choosing two different heating rates.

To determine the reaction order n, we need to introduce another equation [12,13]:

$$\phi_m = \frac{P(u_m)}{\exp(-u_m)/u_m^2}. \tag{14}$$

Here, ϕ_m is the conversion factor (ϕ) at T_m, and u_m is E_a/RT_m. And the probabilistic function $P(u_m)$ is defined

$$P(u_m) = -\int_{\infty}^{u_m}\frac{\exp(-u)}{u^2}du. \tag{15}$$

As a result, the relation between α_m and ϕ_m is

$$\alpha_m = 1-\left[1-\left(\frac{n-1}{n}\right)\phi_m\right]^{1/n-1}. \tag{16}$$

The estimation of n is done by the try-and-error method: first, guess the conversion factor (e.g., 0.9440); from Eq. (16), n is calculated; use Eqs. (11) and (12) to calculate E_a and A; plug all into Eq. (7) to produce α; repeat these steps until the convergence is achieved.

As explained in the procedure (Eqs. (11) to (16)), one could avoid a curve fitting of DTG data by choosing PPM in the estimation. It is known that PPM is relatively accurate when it compared to the other methods. Instead, a root finding scheme must be introduced since there are five unknowns and five nonlinear equations involved. The most effective root finder may be a fixed point iteration. Therefore, one may have to be knowledgeable in programming and algorithms to materialize the root finder as well as a keen experimental skill. In addition, there always exists the possibility of run-time error: the more the code is complex, the higher the possibility gets.

To avoid the iteration addressed above, we return to Eq. (6) and substitute it with Coats and Redfern's approximation for $n\neq1$ [10,11]:

$$g(\alpha) \approx \frac{ART^2}{\beta E_a}\left(1-\frac{2RT}{E_a}\right)\exp\left(-\frac{E_a}{RT}\right). \tag{17}$$

And reworking for Eq. (7) results in

$$\ln\left(\frac{1-(1-\alpha)^{1-n}}{T^2(1-n)}\right)=\ln\left[\frac{AR}{\beta E_a}\left(1-\frac{2RT}{E_a}\right)\right]-\left(\frac{E_a}{RT}\right). \quad (18)$$

The application of the Murray and White's expression [20] into Eq. (18) yields

$$\frac{1}{n-1}\left(\frac{1}{(1-\alpha_m)^{n-1}}-1\right)=\frac{ART_m^2}{E_a\beta}\left(1-\frac{2RT_m}{E_a}\right)\exp\left(-\frac{E_a}{RT_m}\right). \quad (19)$$

The following equation is obtained by treating with Eqs. (10) and (19):

$$n(1-\alpha_m)^{n-1}=1+2(n-1)\frac{RT_m}{E_a}. \quad (20)$$

Eq. (20) alludes to the basic assumption taken by the Kissinger such that the reaction order n is a function of only α_m [21]. To eliminate E_a, we combine Eqs. (11) and (20), and obtain

$$\frac{nT_mH_m}{(1-\alpha_m)}=\frac{2(n-1)}{n(1-\alpha_m)^{n-1}-1}. \quad (21)$$

Compared with Eqs. (14) to (16), there is no need for the repeated calculation due to the absence of the undetermined parameter, ϕ. With the values of α_m, T_m, and H_m obtained directly from the DTG curve, Eq. (21) can be solved by the bisection method for n. The activation energy E_a which is independent of β is calculated by plugging the value of n back to Eq. (11), and the pre-exponential factor A is then computed from Eq. (12).

3. Other Approaches

Among the previous researches, Kissinger [17,18] had Eq. (8) rearranged for determining n ($\neq$1) such as

$$n=\frac{(1-\alpha_m)E_a}{\beta RH_m}\exp(I)\exp\left(-\frac{E_a}{RT_m}\right), \quad (22)$$

with the ordinate intercept I defined as

$$I=\ln\left(n(1-\alpha_m)^{n-1}\frac{AR}{E_a}\right). \quad (23)$$

In this method, E_a is the slope of the $1/T_m$ vs. $\ln(\beta/T_m^2)$ plot. According to the analyses of the experimental results, the slope of the plot varies with β, hence n in Eq. (22) is a function of the heating rate.

Ozawa [7] assumed that α, A, E_a and n are independent of temperature, and used Doyle's approximation [22] to simplify Eq. (6) to

$$\log(g(\alpha))\approx\log\left(\frac{AE_a}{R\beta}\right)-2.315-0.4567\frac{E_a}{RT}. \quad (24)$$

By substituting Eq. (24) into the first two terms of Eq. (6) and integrating the resulting equation, the formula for determining n can be obtained.

Friedman [8] applied a logarithm to Eq. (5), and obtained

$$\ln\left(\beta\frac{d\alpha}{dT}\right)=\ln A+n\ln(1-\alpha)-\frac{E_a}{RT}. \quad (25)$$

In this method, the slope of the $\ln(\beta\, d\alpha/dT)$ vs. $1/T$ plot gives $-E_a/R$. The values of n and A are the slope and the intercept of the E_a/RT_0 vs. $\ln(1-\alpha)$ plot where T_0 is the temperature at which $\ln(\beta\, d\alpha/dT)=0$ [5,23].

4. Experiments

A Type III natural gas vehicle composite cylinder (INOCOM Inc., Korea) was purchased. This cylinder is made of the carbon fiber (T700SC-24000-50C, Toray Industries. Inc., Japan) and the resin, a 100:32 blend in weight of epoxy (HPV-2000, AK Chemical, Korea) and hardner (Akamine-0230, AK Chemical, Korea). The manufacturing processes consist of the hoop-and-helical winding of epoxy/carbon fiber on the mandrel, curing, autofrettage, and drying. The first three steps are followed by the manufacturer's routines for the mass production. The curing takes a total of 120 min: at 358 K for the first 60 min and at 393 K for another. In the autofrettage step, cylinder is filled with water up to 45 MPa, which is necessary for extending the cycle life of the cylinder.

However, since the TGA result depends highly on the moisture content, the drying step is most important and the atmospheric condition in the drier should be precisely controlled for the reproducibility of this study. After the purchase, the cylinders are dried for three months at room temperature (25±1 °C) and the relative humidity of 60±3%, no direct sunlight. Consulting the year-average temperature of 10-15 °C and the year-average humidity of 60-75% in Korea (Korea Meteorology Administration), the cylinder is likely to lose a little more moisture (in other word, becoming more combustible) than the merchants from mass production would do. This way, the test results are expected to be used as a safety standard.

After the drying, the cylinder is cut into 240 small pieces of same size. And, out of them, 24 pieces are randomly chosen, in which one carbon fiber epoxy resin sample (55.87±0.31 mg) is taken from each piece. In this way, one cannot recognize the position in the cylinder at which a sample is taken. Again, four samples are randomly chosen, and each of them is used in the TGA test at one heating rate, i.e., 6 different heating rates and 4 tests per a heating rate.

In this study, TGA N-1000 (SINCO, Korea) is used with 99.95%-purity nitrogen as a purge gas (flow rate of 60 ml/min). Experiments are conducted at various heating rates, i.e., β=3, 5, 10, 20, 30, and 40 K/min. The temperature range is set from 300.7 to 1,223.15 K for all cases. No wonder the duration differs from test to test.

RESULTS AND DISCUSSIONS

In Fig. 1(a), the degrees of CFRP decompositions are plotted for the entire temperature range from 300 to 800 K. Fig. 1(b) shows the same data as in Fig. 1(a) in the temperature range from 300 to 600 K. On the ground that the pyrolysis profile shows an obvious difference before and after 600 K, we consider that the pyrolysis takes place in at least two steps: during the first step, specimen loses some portion of epoxy resin and other ingredients such as moisture and volatile organic compounds (VOCs) whose boiling points are much less than that of the epoxy resin; and during the second step, epoxy resin is thermally decomposed. The point of reflection observed around the degree of decomposition of 0.0175 is considered the end of the first step and, simultaneously, the start of the second step.

The VOCs are expected to mainly consist of the epoxy monomers and the curing agent that did not participate in the cross-link reaction (i.e., curing). Such an inference makes physical sense since the evaporation of those uncross-linked materials takes place at a temperature lower than that of the cured things. For example, Park et

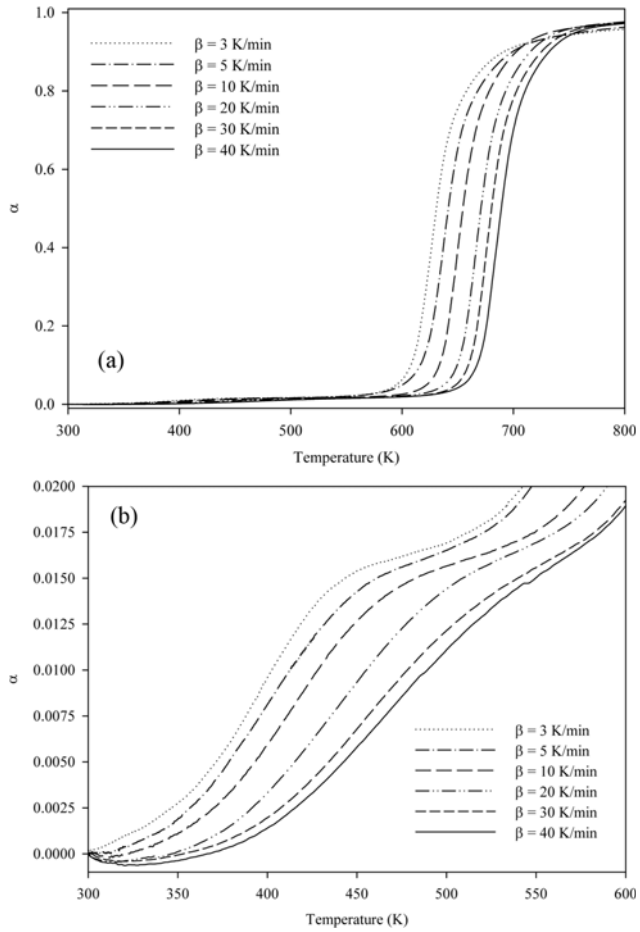

Fig. 1. Results of TGA of CFRP specimen in N_2 environment. The heating rates are set to β=3, 5, 10, 20, 30 and 40 K/min: (a) temperature range from 300 to 800 K covering the entire range; and (b) 300 to 600 K for the first step.

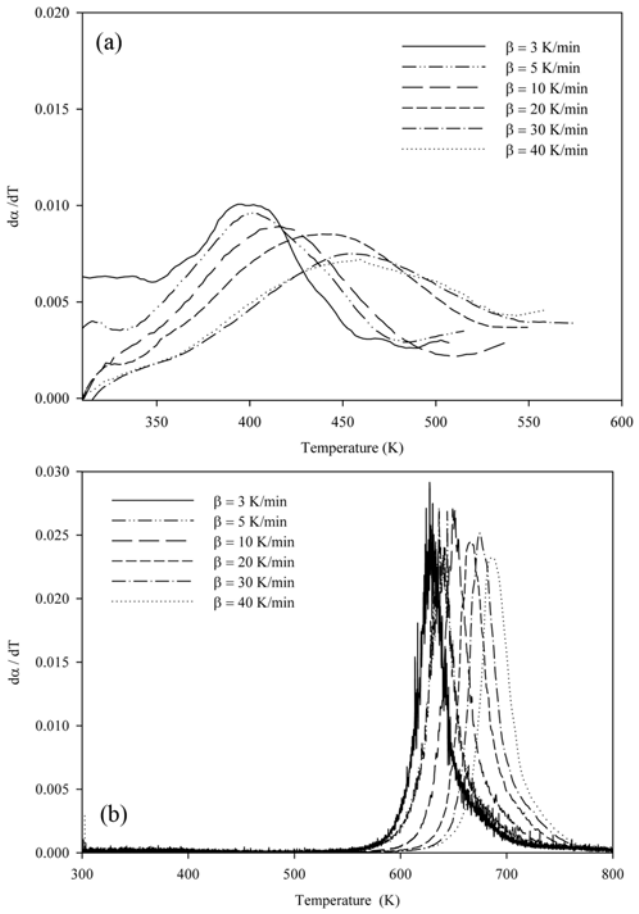

Fig. 2. Results of DTG of the epoxy/carbon fiber composite specimen in N_2 environment: (a) temperature range from 307 to 553 K for the first step; (b) 300 to 800 K for the entire range.

al. reported that the maximum glass transition temperature of Prepreg (DMS2224), which is also made of carbon fiber and epoxy resin, is 456.2 K [4].

The negative values in the conversion shown in Fig. 1(b) are the mechanical but ignorable experimental errors that stem from the initial disturbances due to the supply of nitrogen gas to the chamber in TGA instrument. The magnitude of the error does not exceed 0.01% of the initial sample weight, which is observed with the heating rate of 40 K/min.

The two-step approach has already been employed in the macro-modeling [24]. To be in line with the previous works, in this study, we've independently applied the parameter recovery protocol to the degrees of decomposition in both steps. To apply the modified PPM into the obtained data, the TGA curve should be transformed into a DTG curve as shown in Figs. 2(a) and (b), respectively. In this process, the ordinate in Fig. 1(b), the first step, is rescaled so that 0.0175 (the end point of the first step) becomes 1 in Fig. 2(a). This is because the application of the theoretical model for the temperature derivative of α, see Eq. (5), implies that the completion of the reaction should be set to 1.

In Fig. 2(a), the peaks of pyrolysis rates are located within 390-450 K for all heating rates. It is observed that intensive heating causes a slight decrease in the maximum pyrolysis rate and the increase in position of peak (i.e., 395 to 459 K for β=3 to 40 K/min). In Fig. 2(b), the peaks of pyrolysis rates are located within 625-690 K for all heating rates. It is also observed that the intensive heating causes a slight decrease in the maximum pyrolysis rate and the increase in

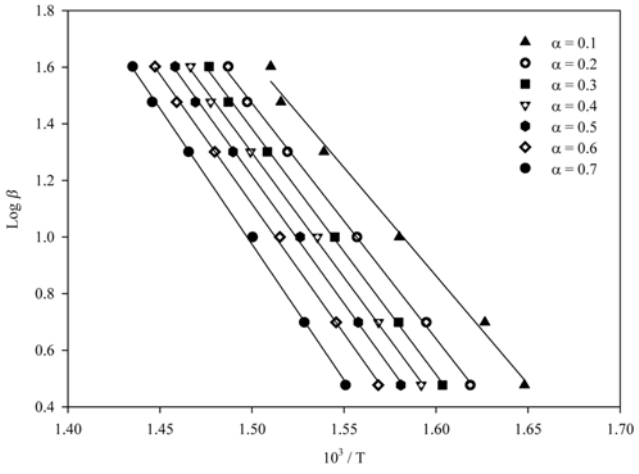

Fig. 3. Plot of logβ vs. 1/T at α=0.1n (n=1, 2, …, 7).

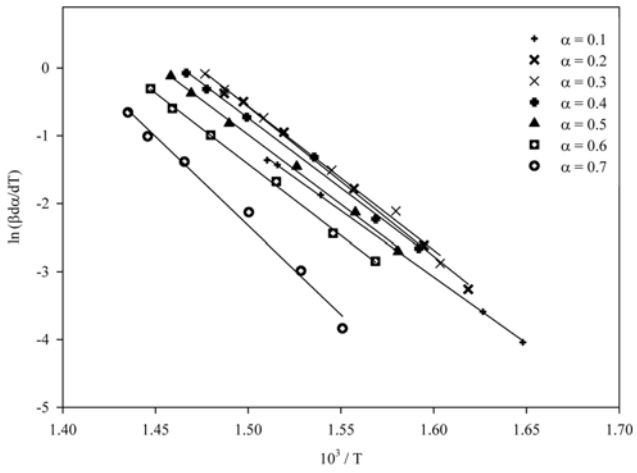

Fig. 4. Plot of ln(βdα/dT) vs. 1/T at α=0.1n (n=1, 2, …, 7).

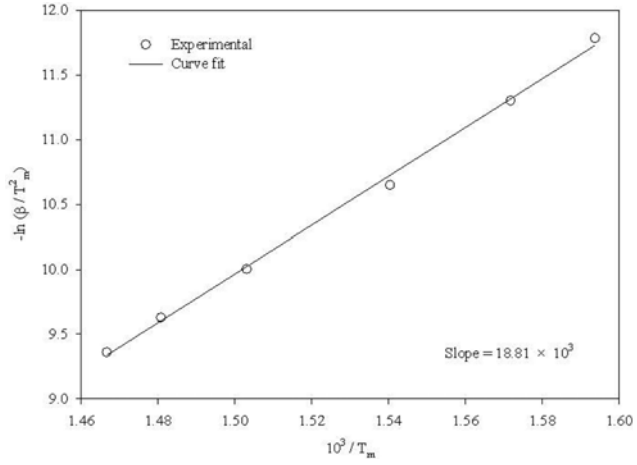

Fig. 5. Plot of $-\ln(\beta/T_m^2)$ vs. $1/T_m$ at β=3, 5, 10, 20, 30 and 40 K/min.

position of peak (i.e., 630 to 683 K for β=3 to 40 K/min).

From estimations of the kinetic parameters by using multi-curve methods, the TGA data shown in Fig. 3 are re-organized according to the Ozawa method into the log β vs. 1/T plot for various values of α. The Friedman and the Kissinger methods are also implemented to analyze the same data in a multiple way producing the $-\ln(\beta d\alpha/dT)$ vs. 1/T plot (Fig. 4) and the $-\ln(\beta/dT_m^2)$ vs. $1/T_m$ plot (Fig. 5), respectively. The results of the parameter recovery by the three methods are listed in Table 1. The mean values of the activation energy E_a are 159 and 179 kJ/mol for the Ozawa and the Friedman methods, respectively.

To test the Coats-Redfern method (a single-curve method), the data for β=10 K/min are selected and used to plot $\ln(g(\alpha)/T^2)$ as a function of 1/T under the assumption of n=2 (see Fig. 6). The slope of the plot is the activation energy E_a. Table 2 contains the results of the parameter recovery by the method. The mean of E_a is 235 kJ/mol. The kinetic parameters obtained by multi-curve methods and by a single-curve method show a great deal of discrepancy, because different assumptions have been applied to different methods. For example, multi-curve methods are based on the assumption that the kinetic parameters do not depend on heating rate, and

Table 1. Kinetic parameters obtained by the multi-curve methods

	α	E_a (J/mol)	R^2	A (min^{-1})	n
Ozawa	0.1	139,273	0.9967	1.32×10^{11}	32.51
	0.2	151,521	0.9994	9.00×10^{11}	11.15
	0.3	158,051	0.9996	2.47×10^{12}	5.55
	0.4	160,263	0.9996	3.07×10^{12}	3.03
	0.5	164,022	0.9995	2.99×10^{12}	1.71
	0.6	166,702	0.9996	6.67×10^{12}	0.95
	0.7	174,459	0.9994	1.16×10^{12}	0.51
Kissinger	-	163,121	0.9971	4.51×10^{12}	1
Friedman	0.1	162,193	0.9998	4.93×10^{10}	1.486
	0.2	182,894	0.9986	1.06×10^{11}	1.189
	0.3	176,068	0.9996	3.04×10^{10}	1.069
	0.4	171,384	0.9970	1.95×10^{10}	1.102
	0.5	170,626	0.9988	2.63×10^{10}	1.209
	0.6	174,426	0.9992	1.21×10^{11}	1.503
	0.7	218,130	0.9937	2.86×10^{14}	2.209

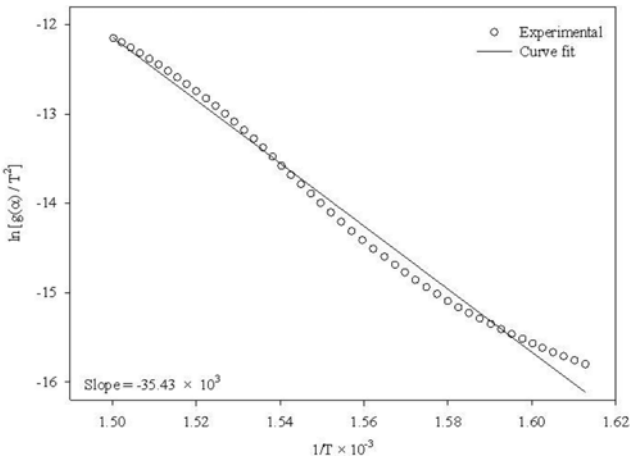

Fig. 6. Plot of $\ln[g(\alpha)/T^2]$ vs. 1/T at β=10 K/min.

Table 2. Kinetic parameters obtained by the Coats-Redfern method (n=2)

$g(\alpha)$	β (K/min)	E_a (J/mol)	R^2	A (min^{-1})
$(1-\alpha)^{-1}-1$	3	203,841	0.9895	1.45×10^{14}
	5	230,813	0.9917	3.11×10^{16}
	10	294,560	0.9946	3.81×10^{21}
	20	329,400	0.9961	1.20×10^{24}
	30	323,200	0.9944	2.25×10^{23}
	40	307,748	0.9961	1.34×10^{22}

thus E_a is determined as a slope of a straight line that is formed by data from experiments with different heating rates [23] (Figs. 3-5). A single-curve method, however, is based on the other assumption that the kinetics does not depend on the decomposition degree, and thus E_a is determined as a slope of a straight line that is formed by data within an experiment [5] (Fig. 6). The multi-curve method can be a good tool to estimate the kinetic parameters for each degree of decomposition, while the results are not as accurate as those by a single-curve method when it is used to test the heating-rate depen-

Table 3. Kinetic parameters obtained by the modified peak property method in the temperature range 307 to 553 K

β (K/min)	T_m (K)	α_m	E_a (J/mol)	H_m	n	A (min^{-1})
3	395.21	0.5200	30,110.4	0.0100	1.108	10.812
5	402.07	0.4959	32,481.1	0.0096	1.270	31.657
10	414.76	0.4736	34,622.5	0.0089	1.427	85.291
20	436.98	0.4553	40,043.6	0.0085	1.615	462.938
30	454.63	0.4335	40,282.8	0.0075	1.761	436.024
40	459.56	0.4154	41,838.1	0.0072	1.940	772.424

Table 4. Kinetic parameters obtained by the modified peak property method in the temperature range 554 to 1,223 K

β (K/min)	T_m (K)	α_m	E_a (J/mol)	H_m	n	A (min^{-1})
3	629.89	0.4396	320,802	0.0218	2.500	1.86×10^{24}
5	638.13	0.4165	353,652	0.0215	2.835	7.35×10^{26}
10	652.18	0.4255	396,608	0.0236	2.730	1.04×10^{30}
20	668.46	0.4320	410,795	0.0238	2.639	4.46×10^{30}
30	677.06	0.4335	429,141	0.0243	2.625	6.94×10^{31}
40	682.79	0.4276	410,602	0.0225	2.695	1.75×10^{30}

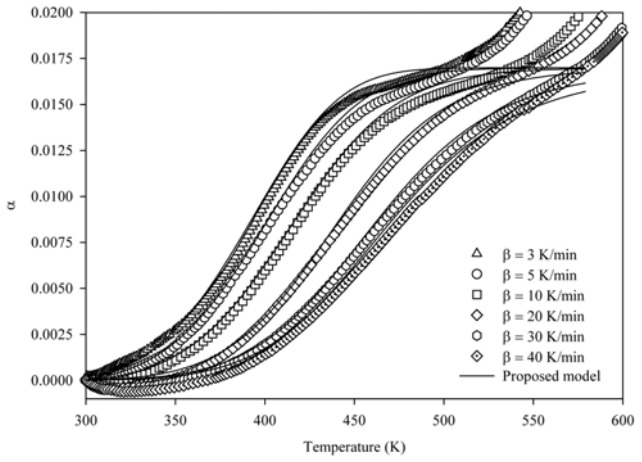

Fig. 7. Model-based predictions of the TGA data by the modified PPM. The data in the temperature range 307 to 553 K are used.

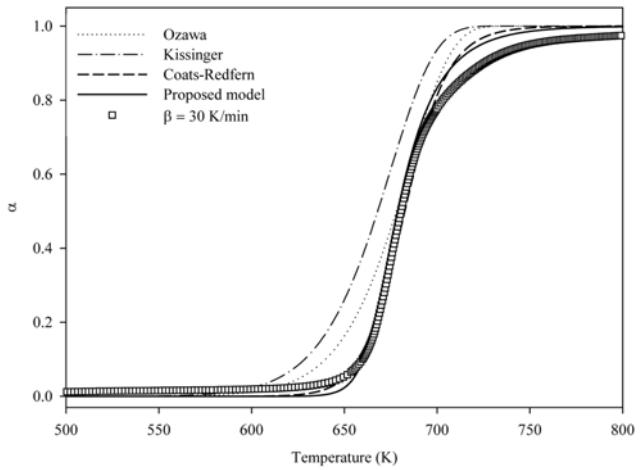

Fig. 8. Results of model-based predictions of TGA test results obtained with (30 K/min).

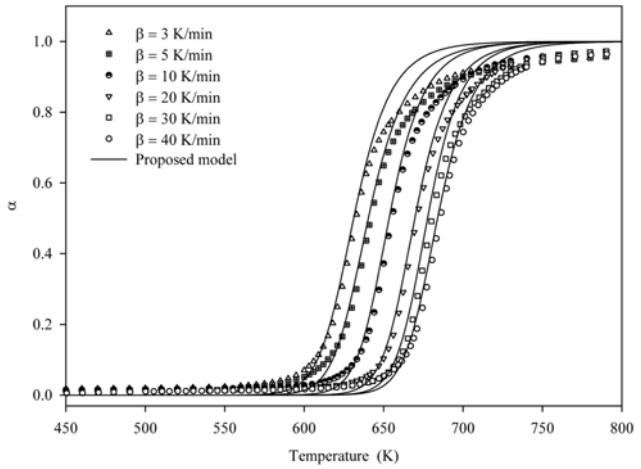

Fig. 9. Model-based predictions of the TGA data by the modified PPM. The data in the temperature range 554 to 1,223 K are used.

dency of the parameters. On the other hand, a single-curve method provides a convenient computation while there is a concern that the reaction order is determined arbitrarily and does not come from experimental data.

Table 3 shows the kinetic parameters obtained by analyzing DTG curve of the first step of pyrolysis (T<553 K). The results are plugged back into Eq. (5) to compare the pyrolysis profile with the experimental observations (Fig. 7). The pyrolysis takes place at the temperature of 488, 501, 517, 525, 538 and 553 K for the heating rates 3, 5, 10, 20, 30, 40 K/min.

Ignition temperature is defined as the temperature at which the concentration of VOCs becomes above the lower flammable limit. In the previous work [24], the specimen of the same kind as used here has been analyzed in the cone calorimeter with radiant heat flux of 50 kW/m^2. There, the ignition temperature was in the range of 492.8 to 628.5 K, which is in accordance with the results of our experiment, i.e., 488-553 K, where TGA is used under a nitrogen environment.

Table 4 contains the kinetic parameters obtained by applying the modified PPM to the data for the second step (554 K<T<1,223 K). The means of the activation energy and the reaction order are 387 kJ/mol and 2.67, respectively. Fig. 8 is prepared to compare the goodness of the methods that have been used so far in this work. There, the data with 30 K/min is used in the range of 600 to 800 K. As a result, the modified peak property model shows the best agreement with the experimental data. Therefore, we apply the modified peak property model to other sets of data, and draw the pyrolysis profiles for them in Fig. 9. As seen in Fig. 9, although there are small discrepancies above α=0.75, the model can be a good estimator of the pyrolysis kinetics of the carbon-fiber composite materials. For α> 0.75, the formation of char crust layer and the lack of VOCs, which

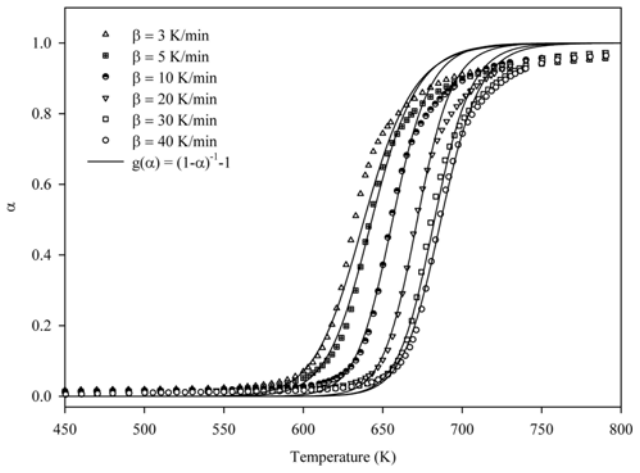

Fig. 10. Model-based predictions of the TGA data by the Coats-Redfern method (n=2).

are not considered in any mathematical model treated here, decelerate the pyrolysis, and this causes the discrepancy. However, in general, the modified peak property model can provide a convenient and effective way to predict the TGA data and to recover the kinetic parameters of the pyrolysis of composite materials. It is noted that, in Fig. 8, the Coats-Redfern method also gives a good estimation to an extent. To compare the goodness with that of the modified peak property model, the Coats-Redfern method is also applied to data with all other heating rates producing Fig. 10. According to Fig. 10, the Coats-Redfern method may be a good estimator for the pyrolysis profile of the composite materials. However, considerable error is observed in the prediction of the data with β=3 K/min.

Finally, it is noted that the potential application of the current study is the modeling and simulation of the surface recession dynamics of a composite cylinder. In the system, whole thickness of a cylinder is classified by two layers: the outer layer in contact with atmosphere and exposed to heat consists of char and VOCs; and the inner layer is made up of only virgin composite materials (i.e., unburnt). The interface of the layers is at the ignition temperature of the composite material [25,26]. The kinetic parameters are used to set up a moving boundary condition of the simulation. Moreover, the current analysis deals with the decomposition kinetic parameters in both cases: pyrolysis before the temperature of a specimen reaches the ignition temperature; and pyrolysis after the temperature of a specimen reaches the ignition temperature. This facilitates a dynamic model where pyrolysis takes place all over the thickness, which may provide more realistic simulation.

CONCLUSIONS

The thermal decomposition kinetics, such as the activation energy E_a, the reaction order n, and the pre-exponential factor A of CFRP, has been investigated by applying the modified PPM, which we propose here, and other types of methods to the experimental results. The pyrolysis experiments for composite materials were performed using TGA with diversity of heating rates. As a result, the modified PPM shows the best performance in predicting the experimental data: it does not require a curve fitting of the data nor a long iterative computation. Consequently, one does not need to struggle with building up the computer program to find roots of set of non-linear algebraic equations. In addition, the modified PPM fits the data well for all range of heating rates used in the experiments.

The results obtained so far can provide the fundamental knowledge in the prediction of the dynamics of the surface recession in the composite cylinder. Especially, as for Figs. 7 and 9, the analyses are performed not only for the pyrolysis when the temperature is less than the ignition temperature (Fig. 7), but also for the pyrolysis when the temperature is greater than the ignition temperature (Fig. 9).

NOMENCLATURE

A : overall pre-exponential factor [min^{-1}]
E_a : activation energy [J mol^{-1}]
H : peak height [-]
m : mass [g]
n : reaction order [-]
R : universal gas constant [8.314 $Jmol^{-1}$ K^{-1}]
T : temperature [K]
t : time [min]

Greek Letters

α : degree of decomposition [-]
β : heating rate [K/min]

Subscripts

f : final
i : initial
m : maximum
∞ : ambient

REFERENCES

1. S. S. Sandhu, *J. Mater. Sci. Lett.*, **15**, 203 (1996).
2. K. A. Trick, T. E. Saliba and S. S Sandhu, *Carbon*, **35**, 393 (1997).
3. N. Regnier and S. Fontaine, *J. Therm. Anal. Calori.*, **64**, 789 (2001).
4. I. K. Park, D. S. Lee and J. D. Nam, *J. Appl. Poly. Sci.*, **84**, 144 (2002).
5. B. Yu, V. Till and K. Thomas, *Compos. Sci. Technol.*, **67**, 3098 (2007).
6. M. K. Seo and S. J. Park, *Korean Chem. Eng. Res.*, **43**, 401 (2005).
7. T. Ozawa, *Trans. Bull. Chem. Soc. Jap.*, **38**, 1881 (1965).
8. H. L. Friedman, *J. Polym. Sci. Part C*, **6**, 183 (1965).
9. H. E. Kissinger, *J. Res. Nat. Bure. Stand.*, **57**, 217 (1956).
10. A. W. Coats and J. P. Redfern, *Nature*, **201**, 68 (1964).
11. A. W. Coats and J. P. Redfern, *J. Polym. Sci. Part B: Polym. Lett. Edn.*, **3**, 917 (1965).
12. S. D. Kim and J. K. Park, *Thermochim. Acta*, **264**, 137 (1995).
13. S. D. Kim and H. D. Chun, *Korean J. Chem. Eng.*, **12**, 448 (1995).
14. H. Chen, N. Liu and W. Fan, *Polym. Degrad. Stabil.*, **91**, 1726 (2006).
15. S. D. Kim, E. S. Jang, D. H. Shin and K. H. Lee, *Polym. Degrad. Stabil.*, **85**, 799 (2004).
16. E. S. Jang, S. D. Kim, D. H. Shin and K. H. Lee, *Korean Chem. Eng. Res.*, **42**, 280 (2004).
17. X. G. Li and M. R. Huang, *Polym. Degrad. Stabil.*, **64**, 81 (1999).
18. P. Ptáček, F. Šoukal, T. Opravil, J. Havlica and J. Brandštetr, *Powd. Technol.*, **208**, 20 (2011).
19. J. H. Flynn and L. A. Wall, *J. Res. Nat. Bure. Stand.*, **70A**, 487 (1966).

20. P. Murray and J. White, *Trans. Brit. Ceram. Soc.*, **54**, 204 (1955).
21. H. E. Kissinger, *Anal. Chem.*, **29**, 1702 (1957).
22. C. D. Doyle, *J. Appl. Polym. Sci.*, **5**, 285 (1961).
23. J. Y. Lee, M. J. Kim and S. W. Kim, *J. Appl. Polym. Sci.*, **81**, 479 (2001).
24. J. H. Lee, K. S. Kim and H. Kim, *Korean J. Chem. Eng.*, **29**, 1508 (2012).
25. J. E. J. Staggs, *Polym. Degrad. Stabil.*, **82**, 297 (2003).
26. W. C. Park, A. Atreya and H. R. Baum, *Combust. Inst.*, **32**, 2471 (2009).